Chapter 4

Theory and Technology of Direct Laser Deposition

Gleb Turichin and Olga Klimova-Korsmik

Additional information is available at the end of the chapter

http://dx.doi.org/10.5772/intechopen.76860

Abstract

Presently the additive technologies in manufacturing are widely developed in all industrialized countries. Replacing the traditional technology of casting and machining with additive technologies, one can significantly reduce material consumption and labor costs. They also allow obtaining products with desired properties. The most promising for manufacturing large-sized products is the additive technology of high-speed direct laser deposition. Using this technology allows to create complex parts and construction to one technological operation without using addition equipment and tools. This technology allows decreasing of consumption of raw materials and decrease amount of waste. Equipment for realization of DLD technology is universal and based on module design principle. DLD is based on layer-by-layer deposition and melting of powder by laser beam from using a sliced 3D computer-aided design (CAD) file. The materials used are powders based on Fe, Ni, and Ti. This chapter presents the results of machine design and research HS DLD technology from various materials.

Keywords: high-speed direct laser deposition, additive manufacturing, stability of process, equipment, structure, properties

1. Introduction

New manufacturing technologies are incorporated into most areas of engineering: aircraft industry, shipbuilding, medicine, engine construction, etc. Existing requirements for its demand are more energy efficient and have environmental compatibility; additive technologies meet both criteria. The intensive development of additive technologies in recent years makes it possible to improve the methods of manufacturing and processing products [1–5]. They allow saving expensive raw materials in comparison with classical production methods, during which up to 90% of the material can be removed. The issue of cost reduction is

especially relevant in knowledge-based industries (gas turbine engine construction, aviation, space exploration, etc.). Selective laser melting (SLM) technology has already been implemented in production in many countries of the world [6, 7]. However, SLM technology is limited by its inability to manufacture large-sized products and low productivity.

The main trend in the development of additive technology is to increase productivity while maintaining the required quality of the product. The most promising technology of product manufacturing is direct laser deposition analogue direct metal deposition (DMD), when the product is formed from a powder, which is supplied by compressed gas-powder jet directly into the laser action zone [8–11]. The jet can be as coaxial and as non-coaxial to focused laser beam, which provides heating and partial melting of the powder and heating the substrate. This technology allows to include a mixture of powders into the gas-powder jet and to change the composition of powders during the process.

The developed technology and equipment have several advantages in comparison with existing analogues. There is a high productivity of DLD process for the manufacture of real parts and products: up to 2.5 kg/h for nickel and iron alloys, up to 1.2 kg/h for titanium alloys. For similar equipment, the productivity is 2–3 times less [12–14]. There are experimental stands with the same high productivity (up to 2 kg/h), preferably [15]. The main feature of the developed equipment is a modular assembly type, which allows to modernize the installation at the customer's request. This is the first Russian technology and equipment for the implementation of additive production.

Complex studies were carried out to understand the relationship between the parameters of the process and the optimization of the technology for obtaining products with specified characteristics. As a result of the research done, the theory and technology of high-speed direct laser deposition are developed. Also a number of machines with various sizes are made for the implementation of this technology. Investigations for powder materials based on iron, nickel, and titanium demonstrated the possibility of obtaining high-quality parts and products. Also, the possibility of working with cermet materials is shown. The research results showed that developed technology of direct laser deposition can replace the currently used technologies, providing multiple increase productivity and material savings, in spite of its technological complexity.

2. Theory of high-speed direct laser deposition

The processes that occur during high-speed laser deposition depend on a large number of distributed parameters which effect on the result [8]. An important aspect of the study is the stability of the direct laser deposition process. Previously, the authors studied the root peak formation in welds during the process of laser welding using highly concentrated energy fluxes. According to the present knowledge about the physical nature of these processes, the

reason for instabilities is self-oscillations of the weld pool [12–19]. Different experimental data confirm this idea [16, 19].

The stability of surface formation in the process of direct laser deposition is determined by the complex of physical processes occurring on the surface of the molten pool, which moves with high speed along the deposited product at a constant flow of matter to its surface. Hydrodynamic stability of melt flow in semiliquid bath, formed by substrate melting under laser beam heating and powder income, depends on driving force, which leads to melt motion. The main driving force for melt motion relative solid substrate in DLD process is Marangoni effect. Therefore velocity of liquid relative solid phase is determined by the rate of the thermocapillary flow [20]. To make the analysis more clear, it is convenient to confine to analyze practically interesting case, when the molten pool length "L" is much greater than its width "b" and depth "H," which depend on parameters of deposition mode. Then analysis of the equation of continuity of the melt allows us to conclude that the "longitudinal" velocity component v_x directed along the axis of the laser beam motion relative to the target is much larger than transverse components v_y and v_z so we the boundary layer like flow. So that equation of the motion can be written in our case as

$$\frac{\partial v_x}{\partial t} + v_x \frac{\partial v_x}{\partial x} = -\frac{1}{\rho}\frac{\partial \rho}{\partial x} + v\frac{\partial^2 v_x}{\partial z^2} \tag{1}$$

At the "bottom" of the molten pool, which coincides with the previous layer surface, the "sticking" condition is fulfilled $v_x|_{z=0} = 0;$ on the surface, the continuity condition of the tangential component of the stress tensor is $\eta \frac{\partial v_x}{\partial z}\Big|_{z=H} = \frac{\partial \sigma}{\partial x}$, where σ is the coefficient of surface tension. Assuming that at the front of the melt pool the surface temperature close to the boiling one and the surface tension value close to "0," taking a linear law for the temperature drop to the "tail" of the melt pool, one can write

$$\eta \frac{\partial v_x}{\partial z}\bigg|_{z=H} = \frac{\sigma}{L} \tag{2}$$

It is possible to get after a number of transformations that with the consideration of Marangoni force, Eq. (1) can be written in the next shape:

$$\frac{\partial v_x}{\partial t} + v_x \frac{\partial v_x}{\partial x} = -\frac{1}{\rho}\frac{\partial \rho}{\partial x} - 3v\frac{v_x}{H^2} + \frac{3\sigma}{2\rho LH} \tag{3}$$

One can use the mass conservation condition to connect the melt velocity v_x with position of the melt pool surface. Let ζ be the height of the perturbation on surface. In our case, the mass flux coming to the melt surface with the gas-powder jet must be taken into account. One can denote the incident mass flux density on melt surface as j (x, ζ). Suppose ζ < < H, it is possible to write the continuity condition of the mass flux as

$$\frac{\partial v_x}{\partial x} \approx -\frac{1}{H}\frac{\partial \zeta}{\partial t} + \frac{j(x,0)}{H\rho} + \frac{1}{H\rho}\frac{\partial j(x)}{\partial x}\zeta. \tag{4}$$

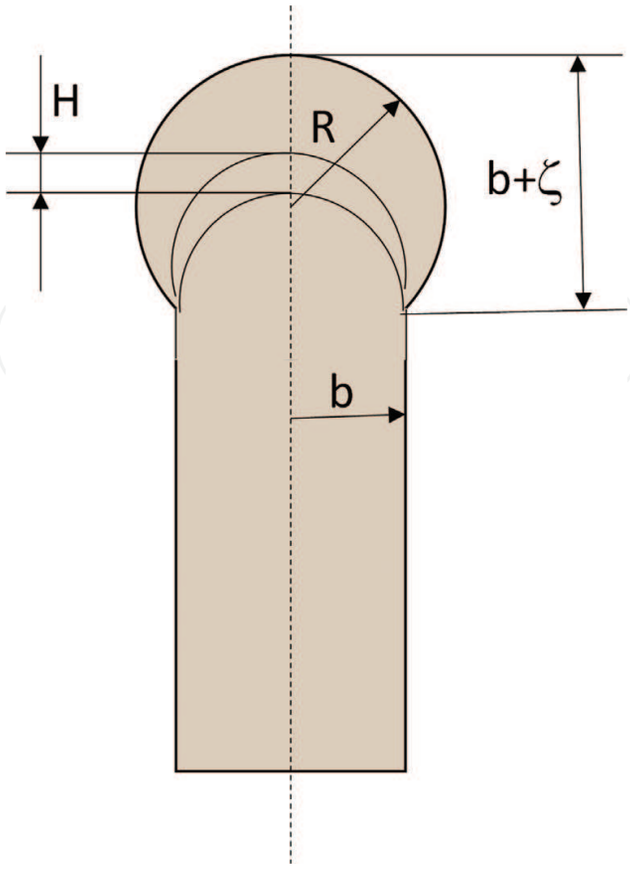

Figure 1. Geometry of the melt pool surface motion.

One can determine the Laplace pressure in the liquid "p" and the additional pressure, which is related to the perturbation of the melt pool surface ζ, taking into account that p = σ/R, where R is the radius of surface curvature (**Figure 1**).

The one-dimensional model of thermocapillary flow does not allow introducing the effects of the influence of grown wall thickness on change in the shape of its surface. For that, we need to introduce a "transverse" dimension. Analysis of term scales in the continuity equation show that melt velocity in "transverse" direction is negligible but pressure changes can be significant. Therefore, when ζ << H, one can get $R \approx b + \frac{\zeta^2}{2b}$, and for pressure it is possible to obtain $p \approx \frac{\sigma}{b} - \frac{\sigma\zeta^2}{2b^3}$.

Considering it, one can write Navier-Stokes equation in the two-dimensional case as

$$\frac{\partial v_x}{\partial t} + v_x \frac{\partial v_x}{\partial x} = -\frac{\sigma}{\rho}\frac{\partial^3 \zeta}{\partial x^3} - 3v\frac{v_x}{H^2} + \frac{3\sigma}{2\rho LH} + \frac{\sigma}{\rho b^3}\frac{\zeta \partial \zeta}{\partial x} \tag{5}$$

In the steady-state approximation, with consideration of mass flux conservation, this equation can be simplified as

$$\frac{\partial^3 \zeta}{\partial x^3} - \frac{\rho {v_0}^2}{\sigma H}\frac{\partial \zeta}{\partial x} = \frac{3}{2LH} - 3v\frac{\rho v_0}{\sigma H^2} - \frac{v_0 j(x,0)}{\sigma H} \tag{6}$$

The boundary conditions for this task are given by $\zeta = 0$ at $x = 0$, $\frac{\partial\zeta}{\partial x}\big|_{x=0} = 0$, $\frac{\partial\zeta}{\partial x}\big|_{x=L} = 0$.

Solution of this problem can be written as

$$\zeta = A\frac{H^2}{G}x + A\left(\frac{H^2}{G}\right)^{3/2}\frac{2 - \exp\sqrt{\frac{G}{H^2}}L - \exp\left(-\sqrt{\frac{G}{H^2}}L\right)}{\exp\sqrt{\frac{G}{H^2}}L - \exp\left(-\sqrt{\frac{G}{H^2}}L\right)} - -A\left(\frac{H^2}{G}\right)^{3/2}$$
$$\frac{1 - \exp\left(-\sqrt{\frac{G}{H^2}}L\right)}{\exp\sqrt{\frac{G}{H^2}}L - \exp\left(-\sqrt{\frac{G}{H^2}}L\right)}\exp\sqrt{\frac{G}{H^2}}x - \tag{7}$$
$$-A\left(\frac{H^2}{G}\right)^{3/2}\frac{1 - \exp\left(\sqrt{\frac{G}{H^2}}L\right)}{\exp\sqrt{\frac{G}{H^2}}L - \exp\left(-\sqrt{\frac{G}{H^2}}L\right)}\exp\left(-\sqrt{\frac{G}{H^2}}x\right)$$

where $G = \frac{\rho {v_0}^2 H}{\sigma}$, $A = -\frac{3}{2LH} + 3v\frac{\rho v_0}{\sigma H^2} + \frac{v_0 j(x,0)}{\sigma H}$.

At the rear part of the melt pool at x = L for the value of ζ, we get

$$\zeta|_{x=L} = A\left(\frac{H^2}{G}\right)^{3/2}\left[\sqrt{G}\frac{L}{H} + 2\frac{1 - Ch\left(\sqrt{G}\frac{L}{H}\right)}{Sh\left(\sqrt{G}\frac{L}{H}\right)}\right] \tag{8}$$

Let us analyze this expression. Depending on the sign of "A," which depends on what is more—underestimation of the surface due to thermocapillary acceleration of the melt flow or its overstating caused by the input of a new material with a gas-powder jet; formation of dimple and humps on melt pool surface is possible. The height of the hump, depending on the speed of the process and the length of the melt pool, can significantly exceed the depth of the melt pool H. Such modes are most dangerous from the point of view of unstable surface formation, but it is impossible to analyze this case using the approximations of the "boundary layer" and the smallness of "ζ." This analysis is a theoretical description of the process of forming the profile of the melt pool surface, taking into account the capillary phenomena and the flow of material that the gas-powder jet brings. For the analysis of nonstationary phenomena leading to instability of the growing process, it is necessary to keep the "nonstationary" terms with time derivatives in the equations and to analyze the stability of the "quasi-stationary" behavior.

We derive an equation describing the dynamic behavior of the local excess of the "ζ" melt pool surface above the "quasi-stationary" surface calculated above. We use the nonstationary Navier-Stokes Eq. (5) and the continuity of the flow Eq. (4) for this purpose. Suppose that

$$\mathrm{v_x}(\mathrm{x}, \mathrm{t}) = \mathrm{v_0}(\mathrm{x}) + \mathrm{v_1}(\mathrm{x}, \mathrm{t}) \tag{9}$$

assuming that $\mathrm{v_1}(\mathrm{x}, \mathrm{t}) \ll \mathrm{v_0}(\mathrm{x})$. Then, obviously,

$$\zeta(x,t) = \zeta(x) + \zeta_1(x,t) \tag{10}$$

where ζ(x) is given by expression Eq. (7). Taking this into account, we obtain from Eq. (10)

$$\frac{\partial v_1}{\partial x} \approx \frac{1}{H}\frac{\partial \zeta_1}{\partial t} + \frac{1}{H\rho}\frac{\partial j(x)}{\partial x}\zeta_1 \tag{11}$$

After substitution of Eqs. (8) and (9) to Eq. (4), taking into account Eq. (10) and the fact that for v_0 and ζ expression Eq. (4) is identity, one can obtain an equation for nonstationary addition for flow velocity:

$$\frac{\partial v_1}{\partial t} + v_0\frac{\partial v_1}{\partial x} + v_1\frac{\partial v_0}{\partial x} = -\frac{\sigma}{\rho}\frac{\partial^3 \zeta_1}{\partial x^3} + \frac{\sigma}{\rho b^3}\frac{\zeta \partial \zeta_1}{\partial x} + \frac{\sigma}{\rho b^3}\frac{\zeta_1 \partial \zeta}{\partial x} - 3v\frac{v_1}{H^2} \tag{12}$$

By differentiating this equation with respect to (x), taking into account Eq. (11), giving similar and neglecting small terms, we arrive to an equation that describes the dynamic behavior of the excess of the growing surface over a stationary value:

$$\frac{\partial^2 \zeta_1}{\partial t^2} = \frac{\sigma H}{\rho}\frac{\partial^4 \zeta_1}{\partial x^4} - \frac{\sigma H^2}{2\rho b^3}\frac{\partial^2 \zeta_1}{\partial x^2} - \frac{\partial \zeta_1}{\partial x}\left(2\frac{\sigma H^2}{\rho b^3 L} - \frac{v_0}{\rho}\frac{\partial j}{\partial z}\right) + \zeta_1\frac{\partial j}{\partial z}\left(\frac{3v}{H^2\rho} + \frac{1}{\rho}\frac{\partial v_0}{\partial x}\right) \tag{13}$$

where L is the length of the melt pool, which is determined from the solution of the heat task.

We use the linear theory of stability and look for the solution of this equation in the form $\zeta_1 = \zeta_0 \exp(i(\omega t - kx))$, where ζ_0 is the constant amplitude and ω in turn can be represented as $\omega = \Omega + i\gamma$, where Ω is the true frequency and γ is the increment (or decrement) of oscillations. Substituting these projects into Eq. (13), we obtain the characteristic equation, which, by neglecting the short-wave capillary ripple in the first approximation, the effect of the viscosity of the melt and the change in its flow velocity due to the thermocapillary effect, we obtain:

$$\Omega \approx \sqrt{\frac{\sigma}{2\rho}}\frac{Hk}{b^{\frac{3}{2}}}, \tag{14}$$

$$\gamma = -\frac{b^{\frac{3}{2}}}{\sqrt{\frac{\sigma}{2\rho}}H}\left(2\frac{\sigma H^2}{\rho b^3 L} - \frac{v_0}{\rho}\frac{\partial j}{\partial z}\right) \tag{14}$$

Thus, we come to the conclusion that, for $\gamma < 0$, an oscillatory instability with frequency Ω and an increment γ occurs at the surface and for $\gamma > 0$ the oscillations will decay with the decrement γ. The condition of stability, obviously, is the fulfillment of the inequality:

$$2\frac{\sigma H^2}{v_0 b^3 L} < \frac{\partial j}{\partial z} \tag{15}$$

Thus, the critical value determining the stability (or instability) of the process of growing is the magnitude of the gradient of the particle flux density in the gas-powder jet along the normal to

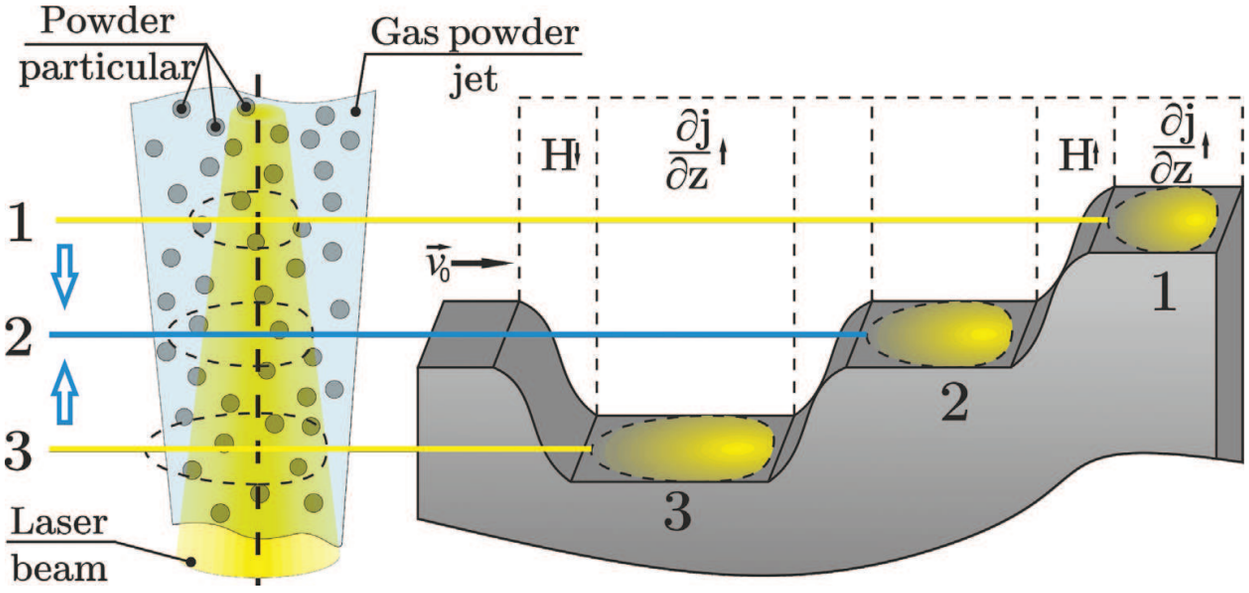

Figure 2. Scheme of stabilization process.

the growing surface. This fact is easy to understand—to stabilize the position of the surface, it is necessary that when it moves upward relative to a stationary value, it would fall under a less dense stream of particles, which would reduce the thickness of the deposited layer, and with shifts downward, under a denser flow, which would increase its thickness and, accordingly, would extinguish the perturbations that arise, as shown in **Figure 2**.

Obviously, for the stability of the process, it is also necessary that the length of the zone in which condition Eq. (15) is satisfied should be greater than the thickness of the layer deposited in one pass. In quantitative analysis, it should also be taken into account that not all particles adhere to the growing surface, so it is necessary to have a gradient value somewhat larger than that given by expression Eq. (15). Thus, a linear analysis of the stability of the process of direct laser deposition process allows us to conclude that stable growth is possible only at the position of the grown surface above the waist of the gas-powder jet, and the necessary condition for stability is the fulfillment of inequality Eq. (15).

3. Technology and equipment of direct laser deposition process

Direct laser deposition technology makes it possible to create complex parts and structures in a single technological step without the use of additional equipment, rigging, and adjustment of equipment [8, 21]. It is a complex technology, which is characterized by a multitude of process parameters. All the variety of parameters can be divided into managed and unmanaged [22]. Managed factors include process parameters such as laser power, nozzle type, traverse speed, powder feeding, spot diameter, layer height, powder fraction, selectable path, and rowing thick walls; it is also necessary to take into account the value of their overlap. Process could proceed in high purity Ar atmosphere for sensitive materials as titanium alloys. Also it is possible to get product under local protective atmosphere for less sensitive materials like some stainless steels. Uncontrollable factors include environmental pressure and other physical

conditions of the environment and quality of the raw powder materials. Especially it is necessary to take into account the thermophysical and technological properties of powder alloys.

Direct laser deposition is a multiparameter process; therefore the results of the process are affected by a complex of technological parameters [8, 23]. Among these parameters, it is possible to identify the main characteristics, which primary determine the course of the process [24]. The basic part of process parameters is described in **Table 1**, where the first four points are the main parameters.

On the basis of theoretical and experimental studies, equipment (**Figure 3**) was developed, which realizes DLD process. This is the first Russian equipment for realization of direct laser deposition technology.

The technology realized with this equipment solves a number of problems for modern engineering, improves process efficiency by 10 times, and reduces the cost of manufacturing parts by 3–5 times. Benefits of implementing the DLD are:

- Productivity of manufacturing parts with complex shapes from intractable materials increases.
- Full automation and "digitalization" of manufacturing.
- Raw material consumption decreases.
- Cost saving.
- Enhancement of technological and engineering capabilities.

The equipment is universal, and based on the principle of modular construction, without using accessory devices and bed structures, it is possible to obtain details of any designs and complexity at the request of the customer. The developed equipment can be operated in a chamber filled with protective gas, which completely eliminates the oxidation of metallic

Process parameters	Productivity	Process stability	Usage rate	Roughness	Depth penetration
Laser power	Minor	Minor	Major	Minor	Major
Spot diameter	Major	Minor	Major	Minor	Major
Traverse speed	Major	Major	Major	Minor	Major
Powder feeding	Major	Major	Minor	Minor	Major
Layer height	Minor	Major	Minor	Major	Minor
Shielding gas rate	—	—	Major	Minor	—
Powder fraction	Minor	—	Major	Major	—
Distance between Nozzle and focus of gas-powder jet	Major	Major	Major	Minor	Minor

Table 1. Process parameters of direct laser deposition technology.

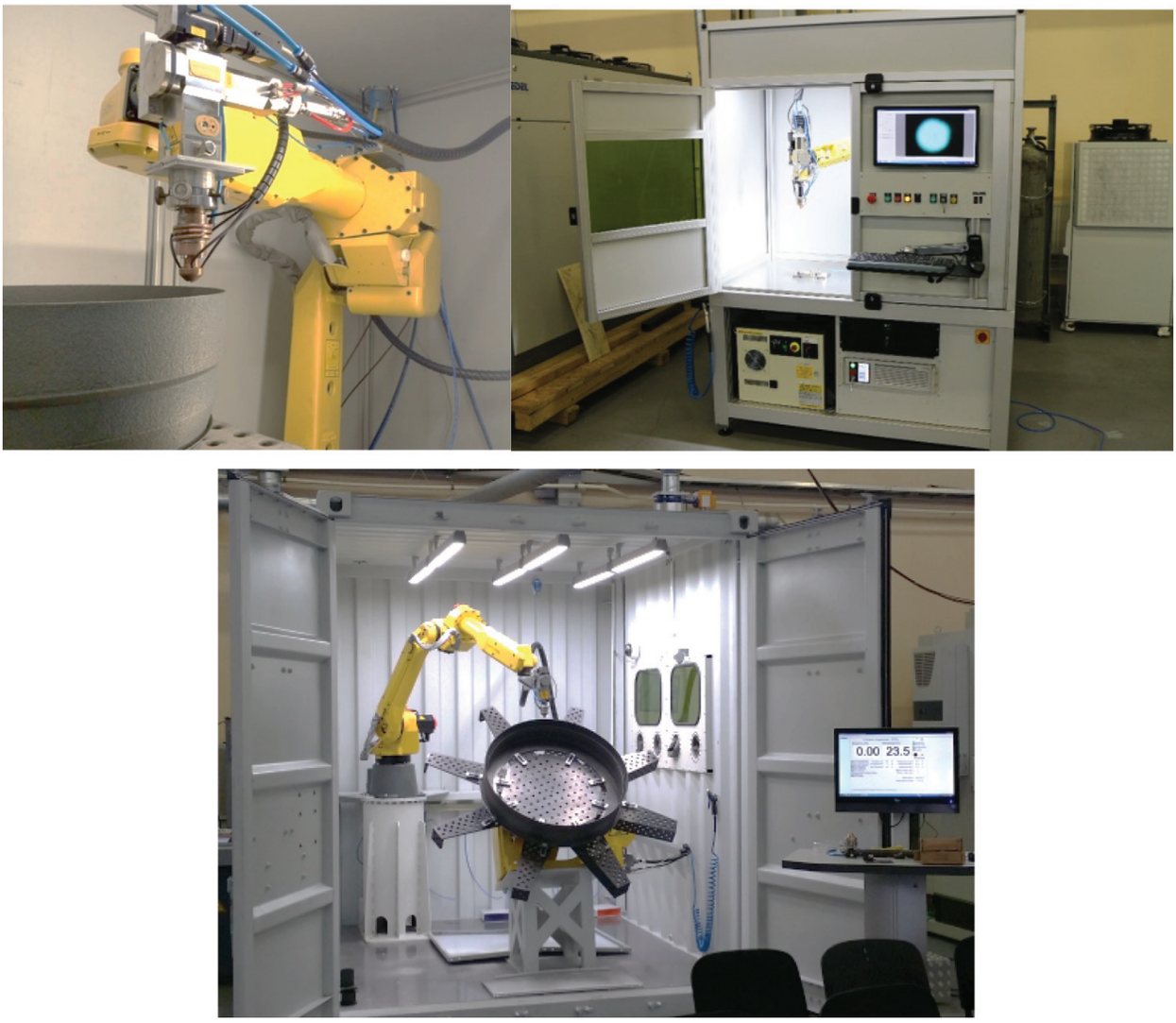

Figure 3. Developed equipment for realization of DLD technology.

materials. A technological tool that combines a laser optical head and a powder nozzle is mounted on an industrial robotic manipulator [23]. As a result, the maximum size of the manufactured product is unlimited. The positioner table used for moving the product is also engaged to increase the technology's capabilities.

During the development of the equipment, special attention was paid to the design of the nozzle [24, 25]. It forms a gas-powder jet and thus has determining effect on DLD process. In the investigations, two types of nozzles were used (**Figure 4**): axisymmetric (or coaxial) and axially asymmetric (lateral or non-axial).

The main disadvantage of the lateral nozzle is shape constancy of deposited layer only in one direction, for example, straight line with moving laser head or the body of rotation with rotating substrate (**Figure 4a**). Therefore, despite its high productivity, it is almost used in the manufacture of equipment. For the developed equipment, the four-jet and annular gap powder nozzles were used.

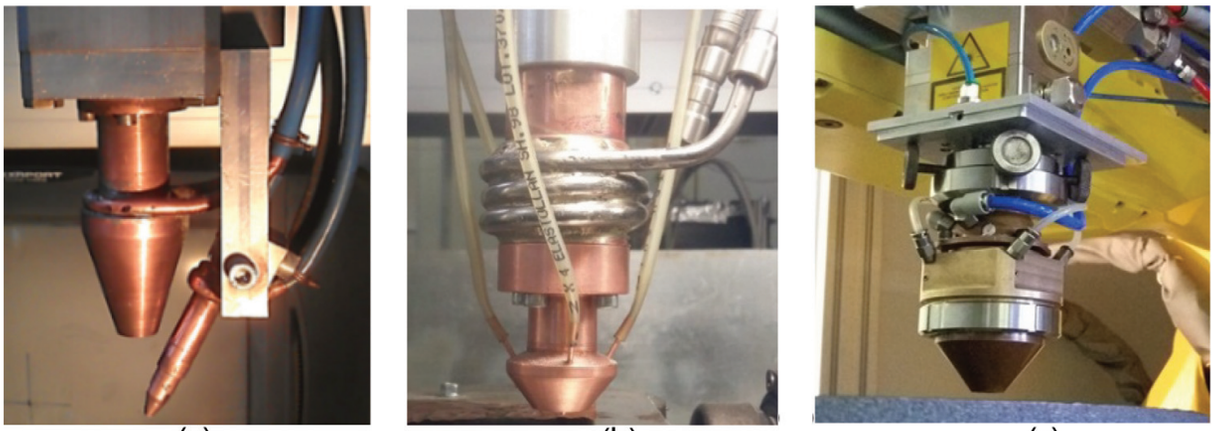

Figure 4. Lateral nozzle (a), coaxial four-jet nozzle (b), and coaxial annular gap nozzle (c).

Technological heads equipped with coaxial nozzles are characterized by independence of technological parameters from the direction of tool movement. This allows using complex processing trajectories and obtaining products with complex geometry. Multiple jet nozzles have from three up to six separate channels, which form powder jets. Its design is more complex but allows more flexibility for powder jet control (**Figure 4b**). During processing, the junction area of jets is located near molten pool, which is formed by a laser beam passing through the central hole of the nozzle. Annular gap nozzles are more technologically advanced (**Figure 4c**). Gas-powder jet is supplied through a gap between two conical surfaces that direct and focus it. Due to the uniform distribution of the powder along the circumference of the annular gap, a high degree of symmetry and isotropy with respect to the direction of motion is achieved. The developed nozzles were used to make a number of machines that realize DLD process.

As a result of the theoretical, technological, and design work, a general principle of constructing the equipment was carried out (**Figure 5**).

Below the components of the complex for the implementation of the direct laser deposition process are listed:

1. The two-axis positioner
2. Working chamber
3. Laser head
4. The robotic manipulator
5. Preparation and supplying gas system
6. Gas cleaning and drying device
7. The fiber laser
8. Chiller

http://dx.doi.org/10.5772/intechopen.76860

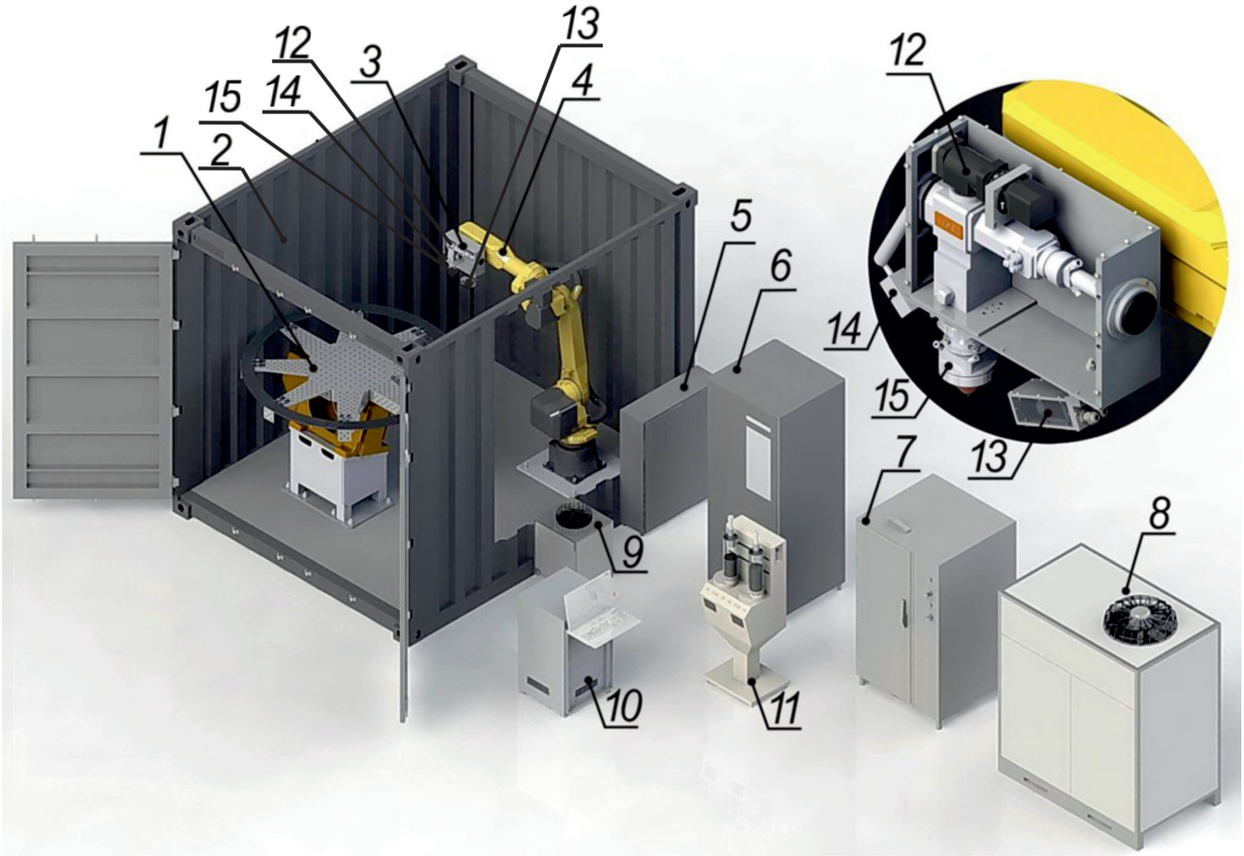

Figure 5. The general scheme of equipment for DLD process implementation.

9. Cooling system

10. Control stand

11. The powder feeder

12. Control system

13. Video surveillance system

14. Monitoring system for processing area

15. Nozzle

The developed technological complex allowed to manufacture products with a traverse speed of up to 60 mm/s and a productivity of 2.5 kg/h.

4. Structure and properties of manufactured products

As a result of the theoretical and experimental studies, the parameters of the process for manufacturing products are carried out, using different metal alloys, which are based on

nickel, iron, and titanium [8, 21, 26, 27]. Using optimal parameters of DLD process allows preparing samples without such macrodefects as cracks and pores (**Figure 6**).

However, in case of violation of the selected modes, porosity, cracks, and lack of fusion may appear. The main reason for the occurrence of large pores (more than 100 μm) is the low quality of the shielding gas or work with local protection. Smaller pores could appear because of low quality of powder [21]. Powders obtained by plasma rotating electrode process (PREP) allow to produce samples of lower porosity as compared with the gas atomization. Powders obtained by gas atomization may contain internal pores. It is also possible for them to form with improperly selected modes, which lead to too high cooling rates. Examples of pores in the samples are shown in **Figure 7**.

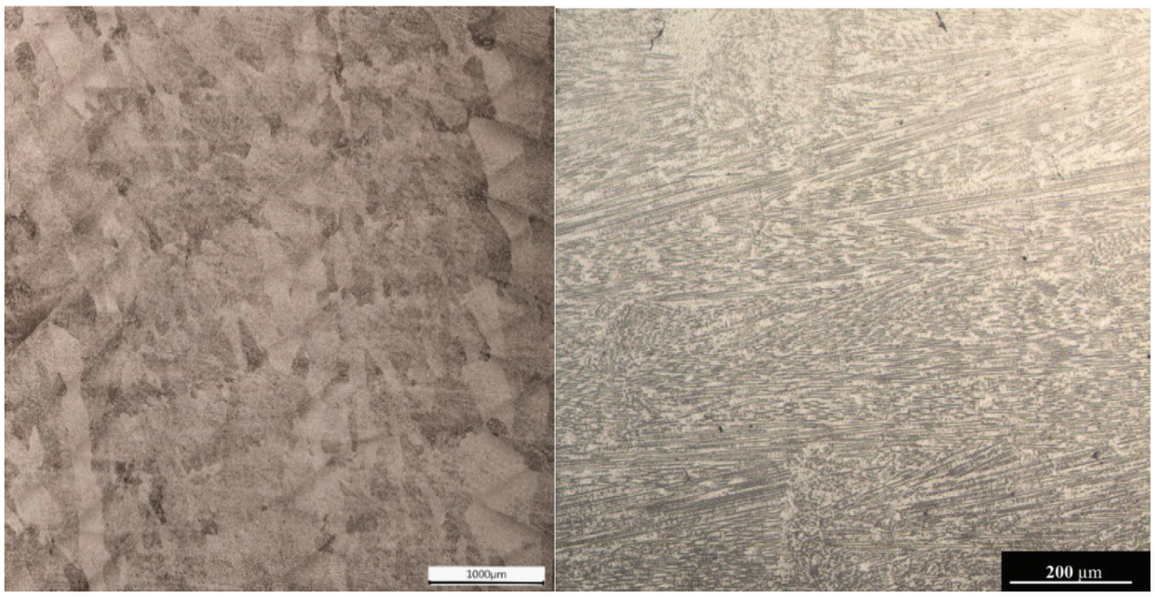

Figure 6. Deposited samples without macrodefects: left—Ti-based alloy and right—Ni-based alloy.

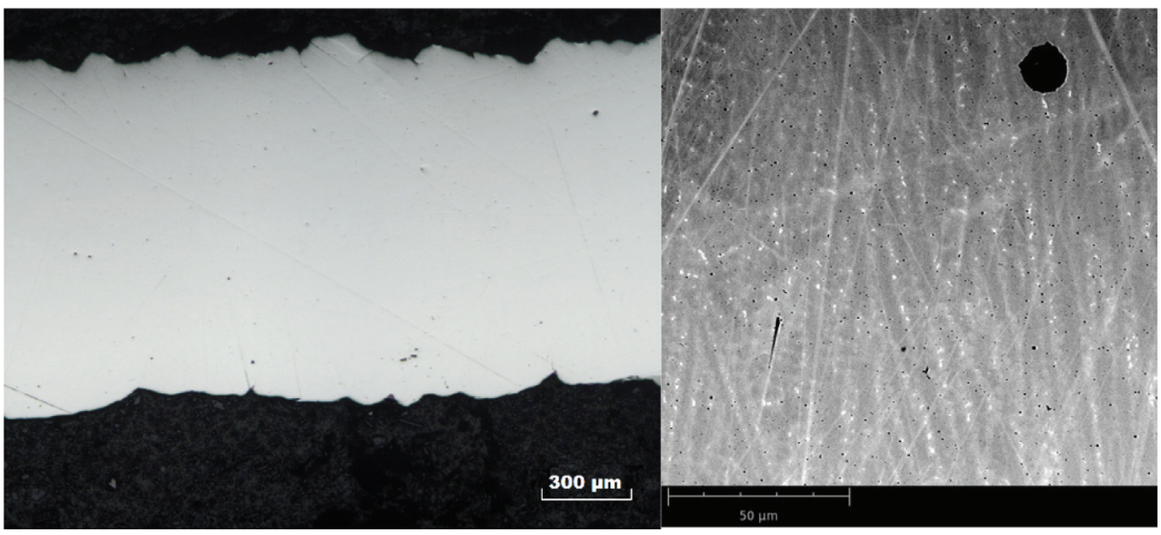

Figure 7. Pores in samples, material Ni-based alloy Inconel 625.

Most often defects are lack of fusion, which have a more negative effect on mechanical characteristics than pores. Small lack of fusion results because of using oxidized powder or contaminated powder. Also, their number increases significantly using local protection, rather than full filling the chamber with shielding gas. Examples of lack of fusion are shown in **Figure 8**.

Lack of fusion is also detected at the deposition of thick-walled products. The appearance of such lack of fusion is due to the lack of energy. They are found in the samples grown at low power, a small size of spot diameter. The size of the overlapping layers also affects, but it has less influence and strongly depends on spot diameter. In **Figure 9** lacks of fusion in thick-walled samples are shown.

In the process of deposition, cracks can also appear, especially in those nickel alloys that are prone to their appearance. For all products obtained by direct laser deposition process, the cracks are an impermissible defect; such products are rejected.

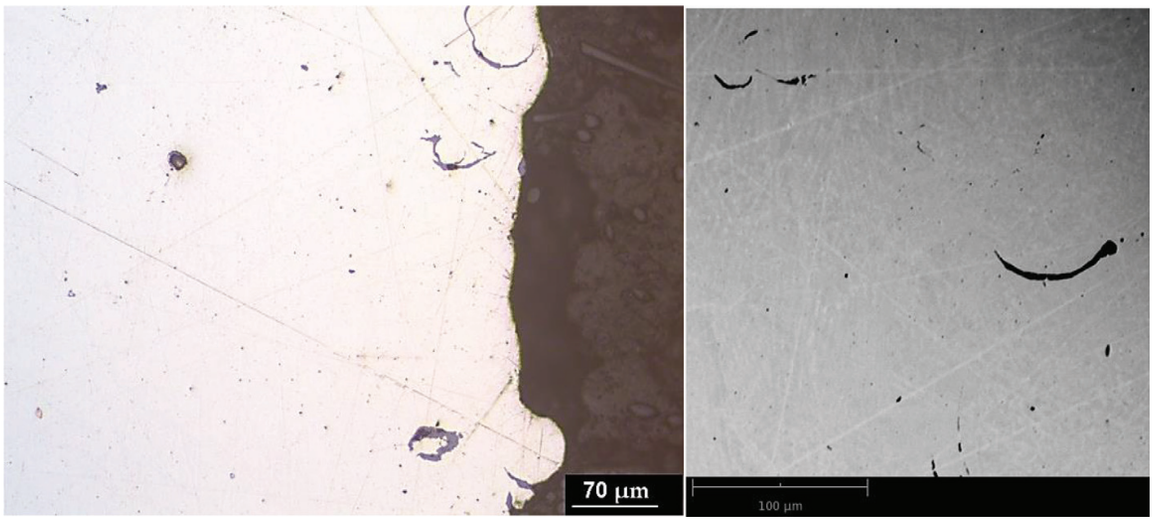

Figure 8. Lacks of fusion in samples, material Ni-based alloy Inconel 625.

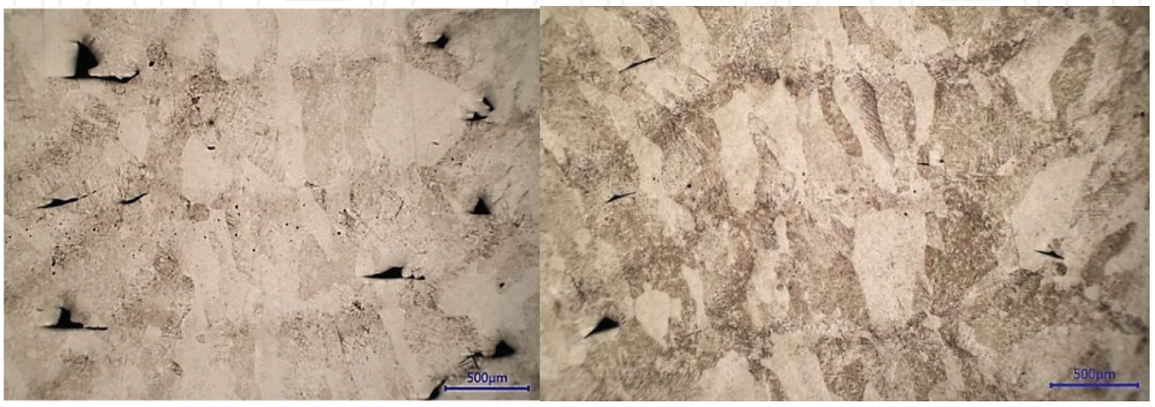

Figure 9. Lacks of fusion in thick-walled sample, material Ti-based alloy Grade 5.

The microstructure of the samples obtained has a finely dispersed, predominantly cast structure. Features of structure formation for the different metal alloys using this technology were studied in detail by the authors. The results of research presented by the

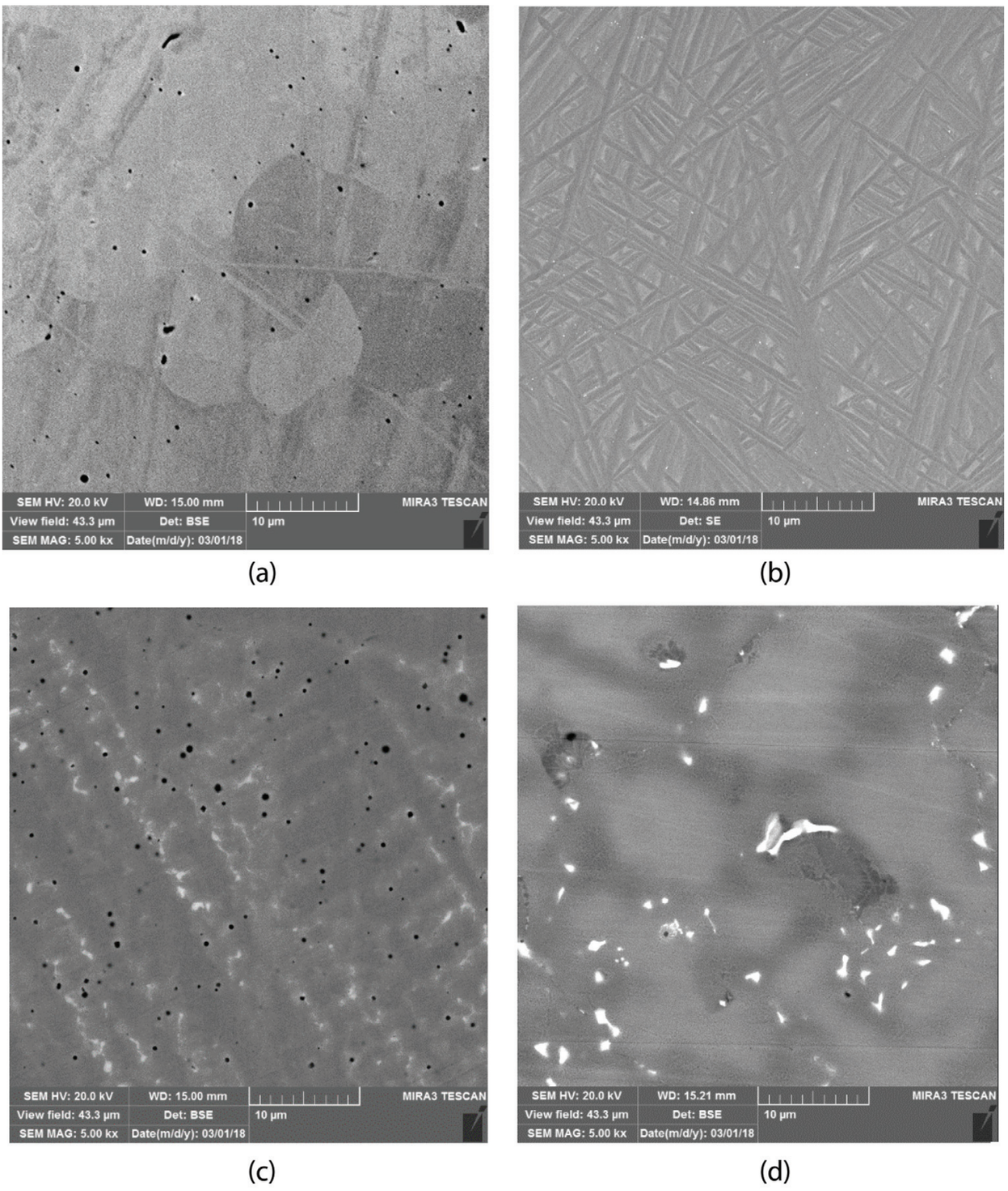

Figure 10. Microstructure of deposited samples: (a) 316 L steel, (b) Ti-based alloy analog Grade 35, (c) Inconel 625, and (d) Ni-based alloy analogue Mar-M200.

Material	Yield strength (0,2% Offset), MPa	Ultimate Tensile strength, MPa	Elongation, %
Inconel 625, DLD	489	865	28.5
Inconel 625, cast [31]	310	800	25
Analogue Mar-M200 alloy, DLD	1046	1353	11.5
Analogue Mar-M200 alloy, cast	1075	1108	2.9
Analogue Grade 35 alloy, DLD	882	968	6.6
Analogue Grade 35 alloy, cast	876	951	6.4
Analogue Grade 5 alloy, DLD	1040	1120	8
Analogue Grade 5 alloy, cast	—	880	4
316 L, DLD	272.5	570	41
316 L, cast [31]	177	441	25

Table 2. Mechanical characteristics of deposited and cast samples.

authors in the articles [26–30]. In **Figure 10** microstructure of different alloys is presented.

Comparing with cast samples, the products that are manufactured by direct laser deposition technology have ultrafine structure. It provides high level of mechanical characteristics (**Table 2**). Mechanical tests were conducted for a greater number of different alloys; the main results are given in **Table 2**. The materials were tested on uniaxial tension; universal testing machine Zwick/Roell Z250 Allround was used.

5. Conclusions

The results of researches show that the developed technology of direct laser deposition, in spite of its technological complexity, can replace the currently used technologies, providing multiple increases in productivity and material saving.

- Direct laser deposition is technology for manufacturing of details with complex form from powder materials using 3D model. It has potential use for different materials in a single part and obtaining details with gradient properties. Using equipment, which realizes this technology, it is possible to produce details of any size.
- The process productivity is 10 times higher in comparison with layered synthesis technologies like SLM. Mechanical properties of the obtained products are much higher than the characteristics of the cast metal; there are no pores and cracks and is no lack of fusion.
- This equipment has a maximum capacity in comparison with existing analogues: up to 2.5 kg/h for metallic materials.
- This is the first Russian technology and equipment for the implementation of additive production.

Author details

Gleb Turichin* and Olga Klimova-Korsmik

*Address all correspondence to: gleb@ltc.ru

State Marine Technical University, Saint-Petersburg, Russian Federation

References

[1] Gu D. New metallic materials development by laser additive manufacturing. In: Surface Engineering. New-York: Elsevier Ltd; 2015. pp. 163-180

[2] Kianiana B, Tavassoli S, Larsson TC. The role of additive manufacturing technology in job creation: An exploratory case study of suppliers of additive manufacturing in Sweden. In: Procedia CIRP, 12th Global Conference on Sustainable Manufacturing—Emerging Potentials, Vol. 26; 2015. pp. 93-98

[3] Gress DR, Kalafsky RV. Geographies of production in 3D: Theoretical and research implications stemming from additive manufacturing. Geoforum. 2015;**60**:43-52

[4] Siemieniuch CE, Sinclair MA, de Henshaw MJC. Global drivers, sustainable manufacturing and systems ergonomics. Applied Ergonomics. 2015;**51**:104-119

[5] Eyers DR, Potter AT. Industrial additive manufacturing: A manufacturing systems perspective. Computers in Industry. 2017;**92–93**:208-218

[6] Liverani E, Toschi S, Ceschini L, Fortunato A. Effect of selective laser melting (SLM) process parameters on microstructure and mechanical properties of 316L austenitic stainless steel. Journal of Materials Processing Technology. 2017;**249**:255-263

[7] Olakanmi EO, Cochrane RF, Dalgarno KW. A review on selective laser sintering/melting (SLS/SLM) of aluminum alloy powders: Processing, microstructure, and properties. Progress in Materials Science. 2015;**74**:401-477

[8] Turichin GA, Klimova OG, Zemlyakov EV, Babkin KD, Kolodyazhnyy DY, Shamray FA, Travyanov AY, Petrovskiy PV. Technological aspects of high speed direct laser deposition based on heterophase powder metallurgy. Physics Procedia. 2015;**78**:397-406

[9] Wilson MJ, Piya C, Shin YC, Zhao F, Ramani K. Remanufacturing of turbine blades by laser direct deposition with its energy and environmental impact analysis. Journal of Cleaner Production. 2014;**80**:170-178

[10] Thompsona SM, Bianc L, Shamsaeia N, Yadollahi A. An overview of direct laser deposition for additive manufacturing; Part I: Transport phenomena, modeling and diagnostics. Additive Manufacturing. 2015;**8**:36-62

[11] Dutta B, Palaniswamy S, Choi J, Song LJ, Mazumder J. Additive manufacturing by direct metal deposition. Advanced Materials & Processing. 2011;**169**:33-36

[12] Renderos M, Girot F, Lamikiz A, Torregaray A, Saintier N. Ni based powder reconditioning and reuse for LMD process. Physics Procedia. 2016;**83**:769-777

[13] Wang Y, Tang H, Fang Y, Wang H. Microstructure and mechanical properties of hybrid fabricated 1Cr12Ni2WMoVNb steel by laser melting deposition. Chinese Journal of Aeronautics. 2013;**26**(2):481-486

[14] Saboori A, Gallo D, Biamino S, Fino P, Lombardi M. An overview of additive manufacturing of titanium components by directed energy deposition: Microstructure and mechanical properties. Applied Sciences. 2017;**7**:883-906

[15] Zhong C, Gasser A, Kittel J, Wissenbach K, Poprawe R. Improvement of material performance of Inconel 718 formed by high deposition-rate laser metal deposition. Materials and Design. 2016;**98**:128-134

[16] Turichin GA. Hydrodynamic stability aspects of gas-vapour channel at energy beam welding. Physics and Chemistry of Metal Treatment. 1996;**4**:74-81

[17] Reisgen U, Schleser M, Abdurakhmanov A, Turichin GA, Valdaytseva EA, Bach F-W, Hassel T, Beniyash A. Study of factors affecting defect formation of the weld seam at electron-beam welding in outer space. Avtomaticheskaya Svarka. 2012;**2**:13-20

[18] Matsunawa A, Kim J-D, Seto N, Mizutani M, Katayama S. Dynamics of keyhole and molten pool in laser welding. Journal of Laser Applications. 1998;**10**(6):247-254

[19] Raisgen U, Schlezer M, Abdurachmanov A, Turichin G, Valdaytseva E, Bach F-W, Hassel T, Banyash A. Investigation of factors influencing the formation of weld defects in non-vacuum electron beam welding. Paton Welding Journal. 2012;**2**:11-18

[20] Kumar A, Roy S. Effect of three-dimensional melt pool convection on process characteristics during laser cladding. Computational Materials Science. 2009;**46**(2):495-506

[21] Glukhov V, Turichin G, Klimova-Korsmik O, Zemlyakov E, Babkin K. Quality management of metal products prepared by high-speed direct laser deposition technology. Key Engineering Materials. 2016;**684**:461-467

[22] Turichin GA, Somonov VV, Klimova OG. Investigation and modeling of the process of formation of the pad weld and its microstructure during laser cladding by radiation of high power fiber laser. Applied Mechanics and Materials. 2014;**682**:160-165

[23] Turichin GA, Somonov VV, Babkin KD, Zemlyakov EV, Klimova OG. High-speed direct laser deposition: Technology, equipment and material. In: IOP Conference Series: Materials Science and Engineering Current Problems and Solutions, Vol. 125; 2016. p. 012009

[24] Turichin G, Zemlyakov E, Klimova O, Babkin K. Hydrodynamic instability in high-speed direct laser deposition for additive manufacturing. Physics Procedia. 2016;**83**:674-683

[25] Korsmik RS, Turichin GA, Babkin KD. Laser cladding technological machine. Investigation of efficiency of various nozzles design. Journal of Physics: Conference Series. 2017; **857**:4

[26] Sklyar MO, Turichin GA, Klimova OG, Zotov OG, Topalov IK. Microstructure of 316L stainless steel components produced by direct laser deposition. Steel in Translation. 2016; **46**(12):883-887

[27] Sklyar MO, Klimova-Korsmik OG, Cheverikin VV. Formation structure and properties of parts from titanium alloys produced by direct laser deposition. Solid State Phenomena. 2017;**265**:535-541

[28] Klimova-Korsmik OG, Turichin GA, Zemlyakov EV, Babkin KD, Travyanov AY, Petrovskiy PV. Structure formation in Ni superalloys during high-speed direct laser deposition. Physics Procedia. 2016;**83**:716-722

[29] Klimova-Korsmik OG, Turichin GA, Zemlyakov EV, Babkin KD, Petrovskiy PV, Travyanov AY. Structure formation in Ni superalloys during high-speed direct laser deposition. Materials Science Forum. 2017;**879**:978-983

[30] Turichin GA, Travyanov AY, Petrovskiy PV, Zemlyakov EV, Kovac M, Vondracek S, Kondratiev A, Khvan AV, Cheverikin VV, Ivanov DO, Bazhenova IA, Dinsdale AT. Prediction of solidification behaviour and microstructure of Ni based alloys obtained by casting and direct additive laser growth. Materials Science and Technology. 2016;**32**(8): 746-751

[31] DebRoy T, Wei HL, Zuback JS, Mukherjee T, Elmer JW, Milewski JO, Beese AM, Wilson-Heid A, De A, Zhang W. Additive manufacturing of metallic components—Process, structure and properties. Progress in Materials Science. 2018;**92**:112-224